processes

MDPI

Article

Opening and Closing Positioning Control of the Seedling Picking-Up Mechanism Based on Fuzzy-PID Control Algorithm

Shuai Han, Weibing Wang *, Yu Wang and Ganghui Liu

College of Mechanical and Electrical Engineering, Shihezi University, Shihezi 832000, China; h1393726393@163.com (S.H.); 13199937910@163.com (Y.W.); uliuganghui@stu.shzu.edu.cn (G.L.)
* Correspondence: wwbshz@163.com; Tel.: +86-132-0109-2272

Abstract: The success rate of automatic transplanter seedling picking is affected by the harsh operating environment of the transplanter and the reduced output accuracy of the opening and closing positioning of the seedling-picking mechanism due to the interference of the external environment. To solve such problems, the paper proposes to use an adaptive fuzzy PID control algorithm as the opening and closing positioning-control system of the seedling-picking mechanism. Based on the theoretical analysis and calculation of the positioning accuracy of the seedling-picking mechanism, a mathematical model of stepper motor angular velocity control was established, and a stepper motor angular velocity control model based on fuzzy PID (conventional PID) control was established in MATLAB/Simulink. In order to further simulate the actual working condition of the seedling-picking mechanism, a simulation model of stepper motor control with disturbance was built, and the response results showed that the fuzzy PID control system could get rid of the disturbance faster under the action of external disturbance signals. The results of the opening and closing positioning test of the seedling-picking mechanism showed that the fuzzy PID control system has higher control accuracy and more stable control performance than the PID control system, which meets the design requirements.

Keywords: transplanter; seedling-picking mechanism; fuzzy PID algorithm; simulation analysis; closed-loop control

check for updates

Citation: Han, S.; Wang, W.; Wang, Y.; Liu, G. Opening and Closing Positioning Control of the Seedling Picking-Up Mechanism Based on Fuzzy-PID Control Algorithm. *Processes* **2022**, *10*, 1349. https://doi.org/10.3390/pr10071349

Academic Editor: Jie Zhang

Received: 25 June 2022
Accepted: 8 July 2022
Published: 11 July 2022

Publisher's Note: MDPI stays neutral with regard to jurisdictional claims in published maps and institutional affiliations.

Copyright: © 2022 by the authors. Licensee MDPI, Basel, Switzerland. This article is an open access article distributed under the terms and conditions of the Creative Commons Attribution (CC BY) license (https://creativecommons.org/licenses/by/4.0/).

1. Introduction

The advantage of pot seedling transplanting technology is that it can effectively avoid the adverse effects of season and weather, to improve the survival rate of pot seedling and increase crop yield [1]. In addition, compared with the traditional manual transplanting and semi-automatic transplanting machine, the automatic transplanting machine has high transplanting efficiency. It also has low labor cost advantages, so the automation of transplanting will be an inevitable trend of development [2]. The seedling-taking device of the automatic transplanter is one of the core components of the transplanter, and the seedling-taking mechanism is also the core component of the seedling-taking device. In the process of clamping seedlings, the opening and closing speed and opening and closing position of the seedling-taking mechanism need to be controlled, and the key lies in the accurate opening and closing positioning of the seedling-taking parts of the seedling-taking mechanism [3].

At present, the research into the power system of the seedling-picking mechanism is mainly in the pneumatic system and the electrical servo system. They mainly control the expansion of the cylinder (the rotation of the motor) to make the seedling-picking mechanism complete the action of pot seedling picking. Hu Jianping et al. [4] designed a control system of whole row picking and interval seeding. The control mode of the solenoid valve and the cylinder corresponded, to realize the action of the seedling-taking mechanism. The characteristic of this control mode was that it could flexibly realize the

action of taking and throwing seedlings in different ways. However, its stability and anti-interference needed to be verified because of the need for telescopic control of the cylinder. Domestic scholars of the automatic transplanter control system research focus on the seedling-feeding device, the seedling-picking device, the planting device, and three or two parts of the coordination of the control, a few focus on the control of each component. At present, few people in China have applied an intelligent control algorithm to the opening and closing positioning-control system of the seedling-picking mechanism to improve the system stability and anti-interference. Ren Ling et al. [5] designed an overall positioning-control system of the seedling-picking mechanism and added the fuzzy PID control algorithm into the overall positioning-control system of the seedling-picking mechanism, realizing the overall precise positioning of the seedling-picking mechanism. Wang Qiao et al. [6] designed a positioning-control system of the seedling tray stepping transportation, which realized the positioning control of the seedling tray stepping transportation and achieved the purpose of coordination and control with the top seedling rod hole tray automatic seedling-taking mechanism. Liu Jiaodi et al. [7] designed a precise positioning-control system for the seedling-replacement device, which integrated the fuzzy PID control algorithm into the control system to achieve the precise positioning of the seedling-replacement device. Wang chao et al. [8] adopted the combination of electric and pneumatic drive way to design a set of transplanting machine automatic control systems. The results of the motion accuracy test of the control system show that the feeding plate position and seedling position error met the operation requirements, that the success rate of the seedling picking could reach 100%, and that the success rate of the seedling throwing was not less than 94.44%. The control performance of the control system was relatively stable. Wei Xinhua et al. [9] based on the combination of PLC controller, sensor, and image acquisition technology, a set of movement coordination control systems of the transplanting machine was designed. Under the action of the control system, the frequency of the seedling selection and seeding could reach 40 plants/min, and the success rate of the seedling selection reached 96.88%. The control performance of the control system was relatively stable, but the control precision of the control system was not considered in the design process. Because the automatic transplanter works in the field environment, it is affected by the ground environment, resulting in vibration, which will affect the seedling-taking mechanism and the positioning error, resulting in the failure of the seedling taking and the seedling leakage, and other problems. In order to solve this kind of problem, it is necessary to design a closed-loop control system as the opening and closing positioning-control system of the seedling-picking mechanism, and the commonly used closed-loop control system is the PID control system. The traditional PID controller has the characteristics of simple structure, being easy to implement, and having good robustness in a certain range. Therefore, it has been widely used in industrial control [10]. However, the conventional PID control system cannot take into account the static and dynamic performance indexes of the system and cannot realize the adaptive adjustment of parameters. Therefore, it can seldom obtain a good control effect in a complex and changeable environment [11]. As an intelligent control, fuzzy control can make timely adjustments to system control parameters according to the system state, so the influence of external interference on the control effect was greatly weakened, and it was especially suitable for nonlinear time-varying objects [12]. The fuzzy control algorithm was combined with the PID control algorithm, and the fuzzy controller was used to real-time self-tuning PID control parameters [13] to achieve accurate and rapid opening and closing positioning control of the seedling-picking mechanism. In addition, the fuzzy control algorithm is easier to establish and implement than the neural network control algorithm, which is also an intelligent control algorithm [14].

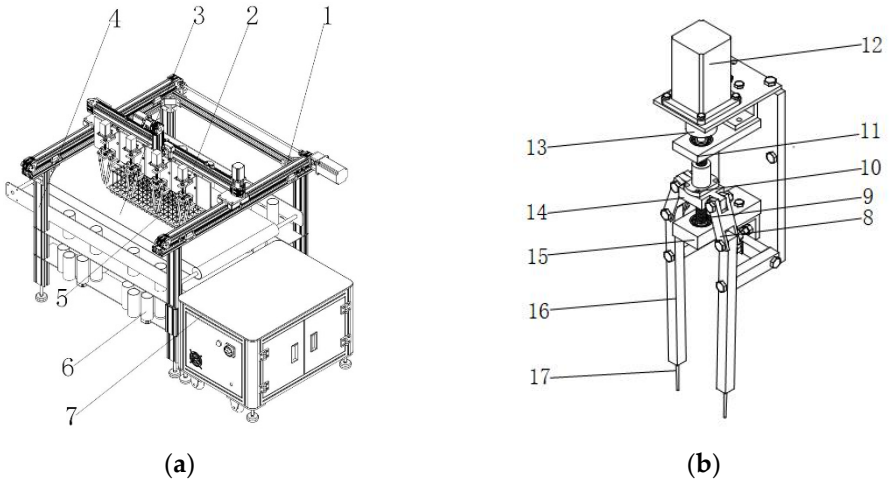
To sum up, the fuzzy PID control algorithm was proposed to design a set of opening and closing positioning-control systems of the seedling-picking mechanism. Fuzzy PID control system was the organic combination of the fuzzy algorithm and the PID algorithm; using the fuzzy algorithm has the advantage of intelligent decision, and making up the PID algorithm can only result in stable control for a specific environment. Comparing with

the control system with a single PID control algorithm, the PID control parameters can be adjusted in real time according to the real-time status of the system, which ensures that the opening and closing positioning-control system of the seedling-picking mechanism has strong anti-interference ability, good stability, and high intelligence.

2. Stepper Positioning-Control System Modeling

2.1. Control Analysis of Seedling Taking Mechanism

The overall structure of the seedling-picking device was shown in Figure 1a. The seedling-picking device was a spaced seedling-picking device, which mainly consisted of a translation module, a seedling-picking mechanism, a seedling tray conveyor, a frame, a potted seedling tray, a catching cup, and a control cabinet. The seedling-picking claw device mainly took 128 hole (16 rows and 8 columns) potted seedlings as the clamping object and clamped 4 potted seedlings each time. Figure 1b showed the seedling-picking mechanism, which was mainly composed of a middle linkage, a screw, a screw nut, an upper bearing seat, a closed-loop stepping motor, a coupling, a nut, a lower bearing seat, a rotating rod, and a seedling needle. When the seedling-picking device was transplanted, the seedling tray was firstly sent to the designated position by the conveyor belt; then, the translating module moved the seedling-picking mechanism to the top of the seedling tray, and the motor started to rotate, driving the screw connected with the motor to rotate, making the screw nut connected with the screw engage in translating movement, and the movement of the screw nut drove the movement of the nut fixedly connected with it, making the intermediate rod connected with the nut rotate and translate. At the same time, the intermediate rod drove the rotating rod connected with it to rotate, and then the seedling-picking mechanism started to pick up seedlings; after the seedlings were picked up, the translation module transported the seedling-picking mechanism to the top of the pick-up cup, and then the seedling-picking mechanism carried out the seedling-dropping operation, which completed a cycle of the seedling picking and -dropping. In the process of taking seedlings, if the seedling-taking mechanism cannot accurately complete the opening and closing positioning control, it may cause empty clips, damage the seedling tray, and affect the next seedling taking cycle, etc. Therefore, the accuracy of the opening and closing positioning of the seedling-taking mechanism directly affected the success rate of the seedling taking.



(**a**) (**b**)

Figure 1. General and partial diagrams. (**a**) Overall construction of the seedling-picking device. (**b**) Seedling pick-up mechanism. (1) Translation module, (2) seedling-collection mechanism, (3) seedling tray conveyor belt, (4) frame, (5) bowl seedling tray, (6) connecting seedling cup, (7) control cabinet, (8) intermediate linkage, (9) screw, (10) screw nut, (11) upper bearing housing, (12) closed loop stepper motor, (13) coupling, (14) nut, (15) lower bearing housing, (16) swivel rod, and (17) seedling pin.

The opening and closing of the seedling-picking mechanism was achieved by the motor driving the screw nut up and down. In order to make real-time correction of the deviation in the process of taking and dropping seedlings, it is necessary to obtain the real-time deviation of the controlled object as the input of the control system, calculate the output control amount through the controller as the input of the actuator [15], and finally achieve the purpose of the real-time correction of deviation. To obtain the deviation amount, it is necessary to obtain the dynamic output of the controlled object and then compare it with the expected value to obtain the deviation value. Here, the closed-loop stepper motor was chosen as the power source of the seedling-taking mechanism, which can obtain the dynamic output of the motor in real time [16] and prepare for the deviation acquisition. The stepper motor is an open-loop control element that converts digital pulse input into rotation output, and its rotation output characteristics depend only on the frequency and number of pulses [17], so the direction of motor rotation can be controlled by controlling the phase sequence of pulses to control the position of the opening and closing of the seedling-picking mechanism. The calculated torque of the seedling-extraction mechanism was not less than 0.045 N.m, and a 57BYG250C stepper motor was selected, whose parameters are shown in Table 1.

Table 1. Parameters of step motor.

Type	Step Angle/(°)	Rated Current/A	Static Torque/N·m	Rotary Inertia /kg·cm^{-2}	Coefficient of Viscosity	Number of Rotor Teeth of Rotary Teeth
57BYG250C	1.8°	3.0	1.8	0.48	0.072	50

2.2. Stepper Motor Angular Speed Control System Modeling

The motor model was a 57BYG250C stepper motor, which was a two-phase hybrid stepper motor, with large torque adjustment range, low noise, and other characteristics. The eddy current loss and the hysteresis effect were ignored in the construction of the stepper motor control system, and its voltage balance equation is shown in Equation (1) [18].

$$\begin{bmatrix} u_a \\ u_b \end{bmatrix} = \begin{bmatrix} R_a & 0 \\ 0 & R_a \end{bmatrix} \begin{bmatrix} i_a \\ i_b \end{bmatrix} + \begin{bmatrix} L_{aa} & L_{ab} \\ L_{ba} & L_{bb} \end{bmatrix} \begin{bmatrix} \frac{di_a}{dt} \\ \frac{di_b}{dt} \end{bmatrix} + \begin{bmatrix} -k_T\omega & 0 \\ 0 & -k_T\omega \end{bmatrix} \begin{bmatrix} \sin(N_r\theta) \\ \sin[N_r(\theta-\lambda)] \end{bmatrix} \quad (1)$$

where u_a, u_b, i_a, i_b are the armature voltage and working current of phase A and B of the motor, respectively, V and A; L_{aa}, L_{ab}, L_{bb}, L_{ba} are self-inductance and mutual inductance of stepper motor A and B phases; R_a and R_b are the winding resistances of A and B phase winding of the motor, Ω; K_T is the back emf coefficient; ω is the rotational speed of the motor, rad/s; Nr is the number of rotor teeth of the motor; t is time, s; θ is the rotation angle, (°); and λ is the pole distance angle, (°). Finally, the motion balance equation of the motor is shown in Equations (2)–(4).

$$T_e = -\frac{1}{2}k_T i_a \sin(N_r\theta) - \frac{1}{2}k_T i_b \sin(N_r\theta - \lambda) \quad (2)$$

$$J\frac{d\omega}{dt} + B\omega + T_L = T_e \quad (3)$$

$$\frac{d\theta}{dt} = \omega \quad (4)$$

where T_e is electromagnetic torque, N·m; J is the moment of inertia, kg/cm^2; B is viscosity coefficient; and T_L is the load torque N·m. Taking the rotational displacement of the motor as the controlled variable, θ_t is the expected rotational displacement, θ_a is the actual rotational displacement, the angle error is $\Delta\theta = \theta_a - \theta_t$, and the control works best

when $\Delta\theta = 0$. Assume that the current in the initial working state is I_0, and the angular displacement and current at the two-phase center $\lambda/2$ are

$$\begin{cases} \theta = \lambda/2 + \Delta\theta \\ i_a = I_0 + \Delta i_a \\ i_b = I_0 + \Delta i_b \end{cases} \tag{5}$$

where I_0 is the rated current, A; and Δi_a and Δi_b are the current deviations of A and B two-phase armature, respectively. It can be concluded from Equations (2)–(5):

$$J\frac{d^2(\Delta\theta)}{dt^2} + B\frac{d(\Delta\theta)}{dt} + k_T I_0 \Delta\theta \cos\frac{N_r\lambda}{2} + k_T I_0 \Delta\theta \cos\frac{N_r\lambda}{4}(\Delta i_a + \Delta i_b) + T_L = 0 \tag{6}$$

When $\lambda = 0$ and $T_L = 0$, Equation (6) is simplified as:

$$J\frac{d^2\theta_a(t)}{dt^2} + B\frac{d\theta_a(t)}{dt} + k_T I_0 N_r \theta_a(t) = k_T I_0 N_r \theta_t(t) \tag{7}$$

At the same time, assuming that the rotational speed of the motor $\omega = \frac{d\theta}{dt}$,$\omega_t$ is the set rotational speed, rad/s; and ω_a is the measured rotational speed of the motor, rad/s. The following equation can be obtained:

$$J\frac{d^2\omega_a(t)}{dt^2} + B\frac{d\omega_a(t)}{dt} + k_T I_0 N_r \omega_a(t) = k_T I_0 N_r \omega_t(t) \tag{8}$$

Take the Laplace transform of Equation (8) and $\omega_a(0) = 0$ to obtain:

$$(s^2 J + sB + k_T I_0 N_r)\omega_a(s) = k_T I_0 N_r \omega_t(s) \tag{9}$$

Finally, the transfer function *G(s)* of the angular velocity control of the stepper motor is:

$$G(s) = \frac{\omega_1(s)}{\omega_0(s)} = \frac{k_T I_0 N_r / J}{s^2 + sB/J + k_T I_0 N_r / J} \tag{10}$$

Substitute motor parameters (Table 1) into Equation (10) to obtain *G(s)*:

$$G(s) = \frac{\omega_1(s)}{\omega_0(s)} = \frac{187.5}{s^2 + 0.15s + 187.5} \tag{11}$$

3. Stepper Positioning Control Algorithm

The control output *u(t)* of the PID control algorithm is:

$$u(t) = k_p e(t) + k_i \int_0^t e(t)dt + k_d \frac{de(t)}{dt} \tag{12}$$

where $e(t)$,$\int_0^t e(t)$,$\frac{de(t)}{dt}$ are the deviation, the integral of the deviation, and the differential of the deviation, respectively; k_p, k_i and k_d are the proportional coefficient, integral coefficient, and differential coefficient of the PID control system, respectively.

The control parameters K_{pf}, K_{if} and K_{df} of the fuzzy PID control system are:

$$\begin{cases} K_{pf} = k_p + \Delta k_p \\ K_{if} = k_i + \Delta k_i \\ K_{df} = k_d + \Delta k_d \end{cases} \tag{13}$$

where Δk_p, Δk_i and Δk_d are the modified values of the PID control parameters.

3.1. Design of Adaptive Fuzzy-PID Control System

The fuzzy controller can be seen as an intelligent decision-making device in a real-time closed-loop control system [19]. By collecting deviations in the control system, the input *u(t)* of the controlled object was determined. The steps of fuzzy controller design were as follows:

(1) Determine the input and output of fuzzy controller and their object theory domain.
(2) Formulate fuzzy rules.
(3) Determine the discrete theory domain of the input and output, and calculate the quantization factor and scale factor.
(4) Set up the simulation model of the fuzzy controller control system.

The block diagram of the fuzzy PID positioning-control system of the seedling-taking mechanism is shown in Figure 2.

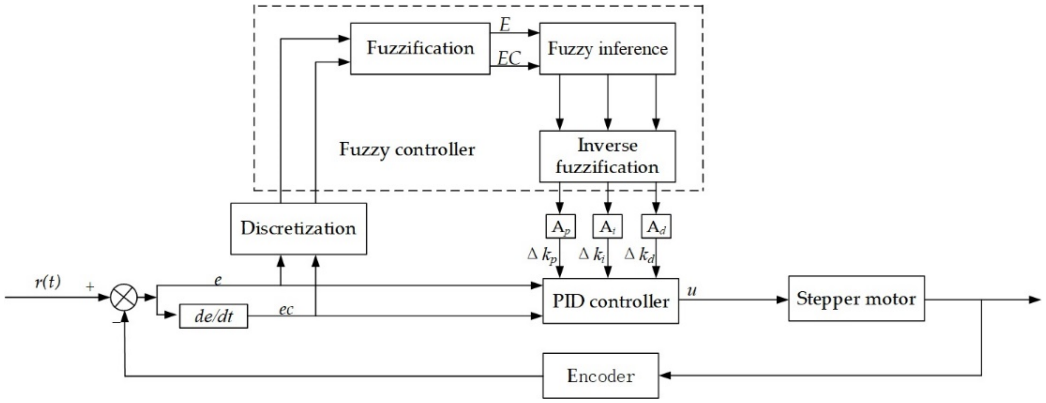


Figure 2. Block diagram of the fuzzy PID control system.

3.1.1. Determination of Membership Functions of Language Variables

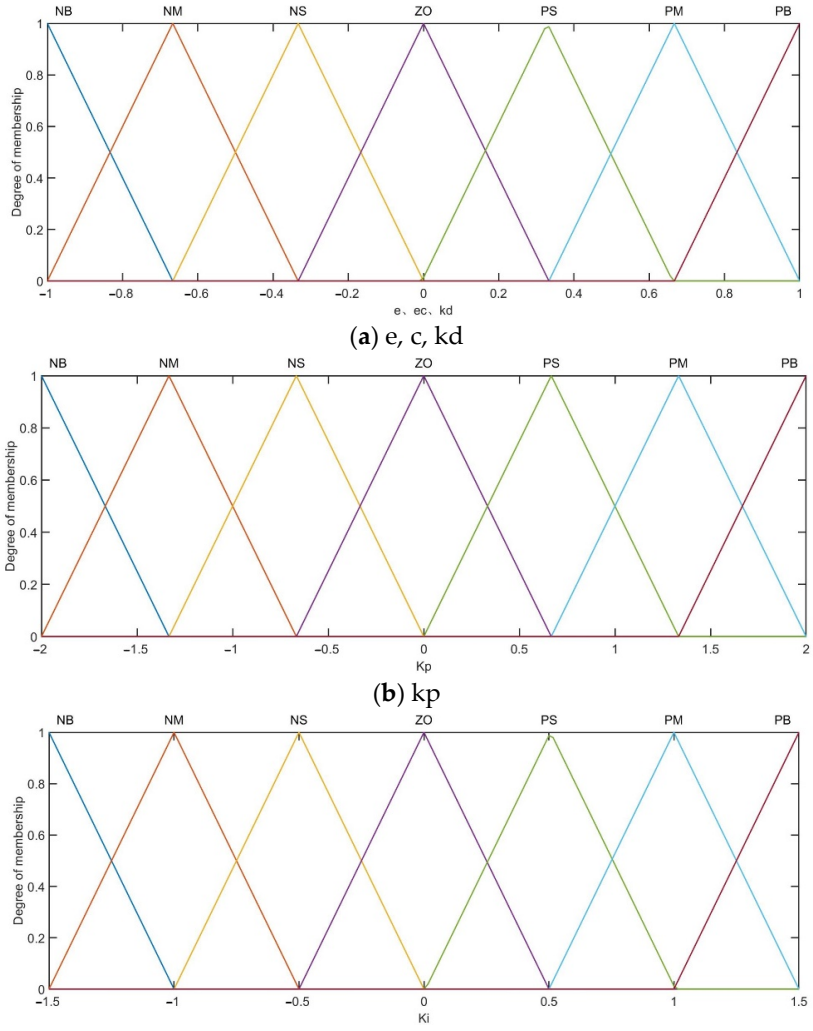
As can be seen from Figure 2, in the fuzzy PID control system, deviation *e* and deviation change rate *ec* were taken as input variables [20], and Δk_p, Δk_i and Δk_d were taken as the output of the fuzzy controller after fuzzification, fuzzy reasoning, and inverse fuzzification. Before fuzzification, the number of elements in the fuzzy set of each input variable should be determined to provide a basis for the subsequent fuzzification and the formulation of fuzzy rules [21]. The fuzzy sets of *e*, *ec*, Δk_p, Δk_i and Δk_d had 7 grades $\{-3, -2, -1, 0, 1, 2, 3\}$, and the corresponding language variables were {negative big (NB), negative medium (NM), negative small (NS), zero (ZO), positive small (PS), positive median (PM), positive big (PB)}. The physical theoretical domain of the motor angular velocity deviation *e* was $[-20/11, 20/11]$; the physical theoretical domain of *ec* was [–100, 100]; and the physical theoretical domain of fuzzy controller outputs Δk_p, Δk_i and Δk_d were $[-1.6, 1.6]$, $[-0.7, 0.7]$, and $[-0.1, 0.1]$ respectively. The corresponding language variables were *KP*, *KI* and *KD*. According to the above conditions, trapezoidal membership function curves were used for input language variables *E* and *EC*, and their discrete theory domains were [–1, 1] and $[-1, 1]$ respectively. Trapezoidal and membership function curves were also used for output language variables *KP*, *KI* and *KD*, and their corresponding discrete theory domains were [–2, 2], $[-1.5, 1.5]$, and [–1, 1] respectively; the membership function curve is shown in Figure 3. The quantization factor *k* and the scale factor *A* are

$$k = \frac{2n}{x_h - x_l} \tag{14}$$

$$A = \frac{x_h - x_l}{a_h - a_l} \tag{15}$$

where $2n$ is the number of intervals divided by the integer elements in the discrete theory domain; and x_h and x_l represent the upper and lower limits of the theoretical domain

of ec, e, Δk_p, Δk_i and $\Delta k_{d,}$ respectively. a_h and a_l represent the upper and lower limits of the discrete theory domain of Δk_p, Δk_i and $\Delta k_{d,}$ respectively. After calculation, ke = 0.55, kec = 0.01, Ap =0.8, Ai = 0.5, and Ad = 0.1.



(**a**) e, c, kd

(**b**) kp

(**c**) ki

Figure 3. Degree of membership graph. (**a**) Membership function graph of e, ec and kd. (**b**) Membership function graph of kp. (**c**) Membership function graph of ki.

3.1.2. Development of Fuzzy Rules for Fuzzy PID Controller

The general form of the fuzzy rule in the fuzzy PID controller was "if A and B then C and D and E" [22]. According to the above form, the different outputs of *KP*, *KI* and *KD* when *E* and *EC* were in different states were obtained by combining expert experience and a large number of experiments [23], as shown in Table 2.

Table 2. Fuzzy PID control rule.

E	***EC***							
	NB		**NB**		**NB**		**NB**	
NB	NB/NM/PM	NB	NB/NM/PM	NB	NB/NM/PM	NB	NB/NM/PM
NM	NS/NS/PS	NM	NS/NS/PS	NM	NS/NS/PS	NM	NS/NS/PS
NS	NM/NS/PS	NS	NM/NS/PS	NS	NM/NS/PS	NS	NM/NS/PS
ZO	PS/PS/ZO	ZO	PS/PS/ZO	ZO	PS/PS/ZO	ZO	PS/PS/ZO
PS	PM/PS/ZO	PS	PM/PS/ZO	PS	PM/PS/ZO	PS	PM/PS/ZO
PM	PM/PM/NS	PM	PM/PM/NS	PM	PM/PM/NS	PM	PM/PM/NS
PB	PB/PB/NB	PB	PB/PB/NB	PB	PB/PB/NB	PB	PB/PB/NB

Based on the input and output of the membership function of the fuzzy PID controller above, the fuzzy control rules [24], and other relevant parameter sets, the output surface of the approximate correction of the PID's proportional coefficient, integral coefficient, and differential coefficient was obtained, as shown in Figure 4

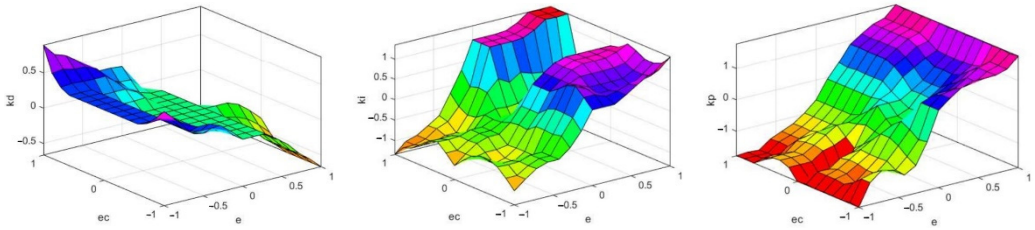


Figure 4. Spatial surface plot of Δk_p, Δk_i, Δk_d approximations.

3.1.3. Fuzzy Reasoning and Inverse Fuzzification in Fuzzy Controller

In this design of the fuzzy PID controller, the Mamdani method [25] was used for fuzzy reasoning. Therefore, according to the fuzzy rules shown above, the fuzzy relations R_p, R_i and R_d formed by the fuzzy theory fields E, EC, KP, KI and KD are

$$R = \bigcup_{1,1}^{m,n} R_{\mathrm{mn}} = \bigcup_{1,1}^{m,n} (\widetilde{R}_{\mathrm{m}}^{T} \circ C_n) \tag{16}$$

$$R_m = E_m^T \times EC_n \tag{17}$$

where $\times$ is the direct product symbol; $\cup$ is the large operator; $\circ$ is the inference symbol; $\widetilde{R}^T$ is the transformation rank of $E_m^T \circ EC_n$ after the inference operation and the transformation into the row vector; and m and n are the number of elements in the fuzzy sets E and EC, respectively, 7,7. When the value of a discrete theory domain was input by the fuzzy controller, the corresponding fuzzy set U_p, U_i, U_d could be obtained after the Mamdani method inference operation:

$$U = (E_m \times EC_n) \circ R \tag{18}$$

A fuzzy subset was obtained after fuzzy reasoning, and a clear value could be output only after inverse fuzzification. Here, the center of gravity method was used in fuzzy decision making [26], and the near-clear values of Δk_p, Δk_i and Δk_d output after fuzzy decision making are:

$$f = \frac{\sum_{i=1}^{p} c^*(i) u_c^*(i)}{\sum_{i=1}^{p} u_c^*(i)} \tag{19}$$

where $c^*(i)$ is the element in the discrete theory domain Δk_p, Δk_i and Δk_d; P is the number of elements in the discrete theory domain of the output fuzzy subset; and $u_c^*(i)$ is the corresponding membership degree of each element in the discrete theory domain of the output fuzzy subset. The clear values Δk_p, Δk_i, and Δk_d of the modified PID controller can be obtained by multiplying the nearly clear values output of the fuzzy controller by their respective scale factor A.

4. Simulation Analysis of Stepper Motor Control System

4.1. Simulation Analysis of Unit Step Response of Control System

The offline adjustment of fixed PID control parameters through the MATLAB/Simulink functional module can improve the design efficiency of the control system to a greater extent [27], and the adjusted PID control parameters k_p, k_i and k_d were determined to be 46, 45, and 1 respectively. After the fuzzy controller was established in the MATLAB/Fuzzy toolbox with the PID control system in Simulink to build the system simulation model of adaptive fuzzy PID control stepper motor, the system simulation model plot shown in

Figure 5 was obtained, and the response curve plot shown in Figure 6 was obtained with the unit step as the input excitation.

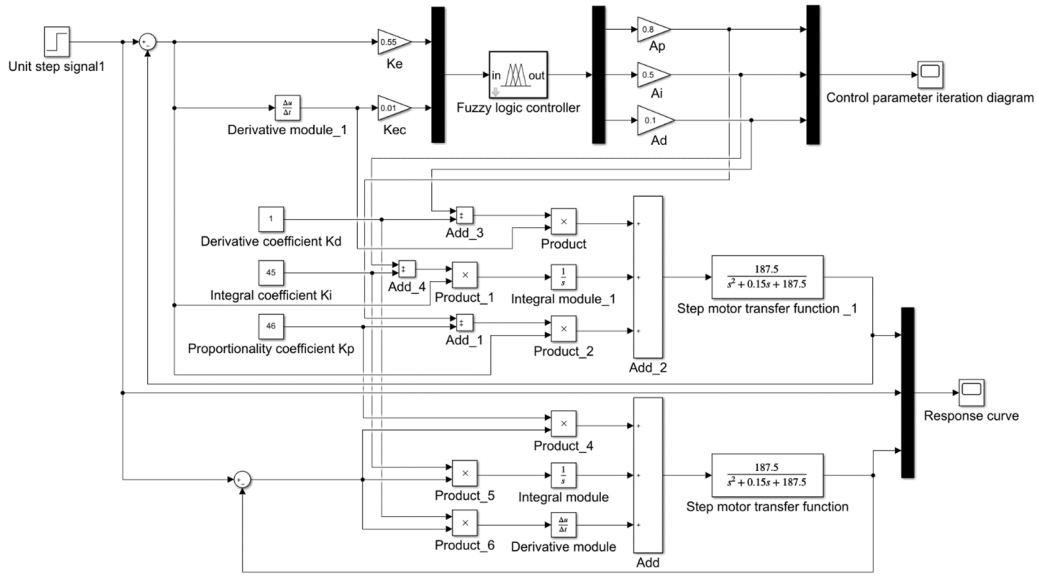


Figure 5. Unit step response simulation model for control systems.

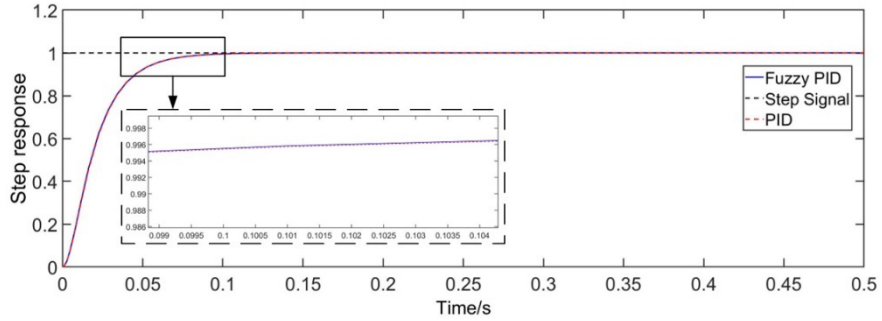


Figure 6. Control system step response graphs.

Figure 6 shows that two kinds of control system of the unit step response curve were no overshoot and no steady-state error, but from the response curve, at the same time, the fuzzy PID response curves were in the upper part of the traditional PID response curve; therefore, the fuzzy PID's response speed is faster than the traditional PID control system; in addition, the simulation results show that the unit step response time of the PID control system to the steady state was 0.152 s, and the unit step response time of the fuzzy PID control system to the steady state was 0.145 s. Compared with the PID control system, the response time of the PID control system to the steady state was shortened by 4.605%. In conclusion, compared with the PID control system, the fuzzy PID control system had a faster unit step response speed, so the control performance of the system was better.

4.2. Control System Responsiveness under Disturbance

Most of the automatic transplanters were used for field transplanting operations, which suffered from the impact of the ground environment, leading to the vibration of the automatic transplanter. The vibration led to the positioning error of the seedling mechanism, which was undoubtedly a severe challenge for its control system. In order to simulate the response performance of the control system to external interference, the unit step signal was added to the interference signal, to compare the response of the two control systems to external interference. The simulation time length was 10 s; the step response signal was input in 0~10 s; the disturbance signal was added in 1~1.3 s; the amplitude was 0.4, generated by the signal generator module; and the frequencies were as follows: the

sawtooth disturbance signals of 3 Hz 10 Hz, 20 Hz, 30 Hz, 40 Hz, and 50 Hz were used to test the response of the control system. The simulation model is shown in Figure 7, and the simulation results are shown in Figure 8. The response time of these two control systems to the steady state is shown in Table 3.

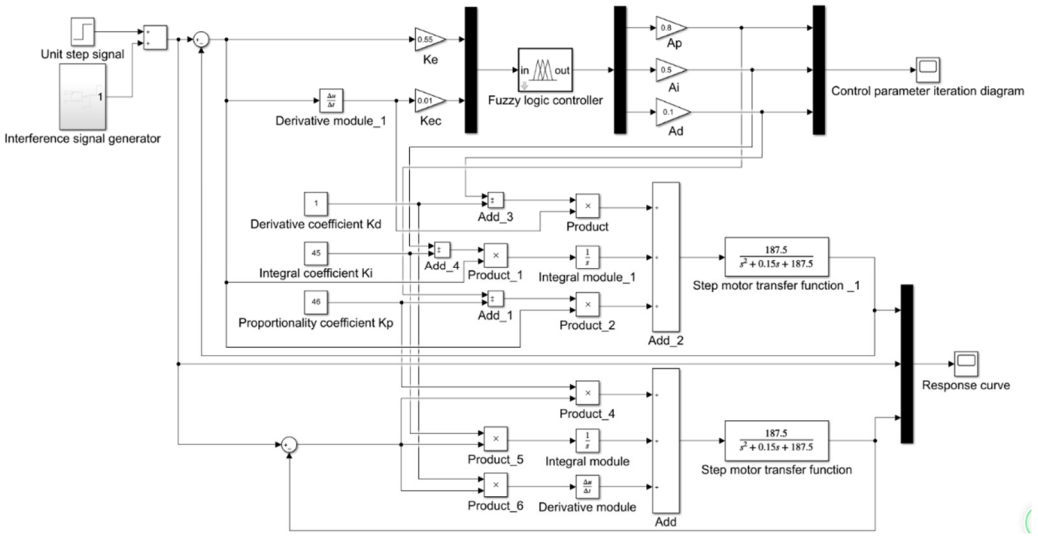
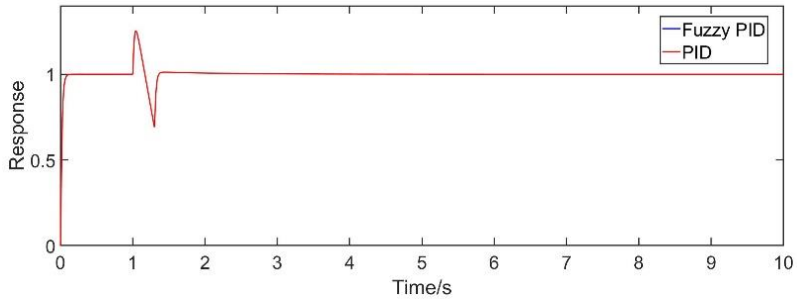


Figure 7. Simulation model of the control system after adding disturbances.

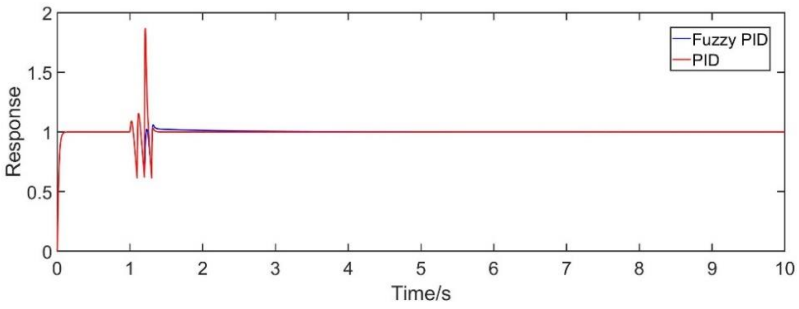
Table 3. Response results of control system.

Response Results of PID Control System		Response Results of Fuzzy PID Control System	
Serial Number	**Frequency of Interference Signal/Hz**	**Time to Steady State/s**	**Percentage Lift/%**
1	3	4.713/4.698	0.318
2	10	5.677/5.358	5.619
3	20	6.402/5.344	16.526
4	30	6.140/5.725	6.157
5	40	4.066/3.784	6.936
6	50	5.648/5.237	7.277

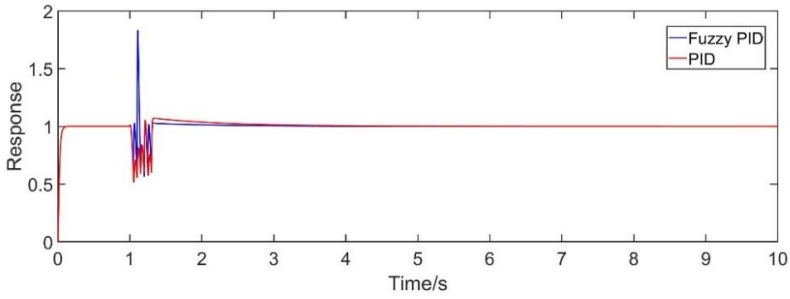
It can be seen from Figure 8 and Table 3 that the response curves between the fuzzy PID control system and the PID control system almost overlap after the addition of 3 Hz interference signal. However, the time for the fuzzy PID control system to reach the steady state was shortened by 0.318% compared with that of the PID control system. After the interference signal with a frequency of 10 Hz was added, the response of the fuzzy PID control system showed no overshoot, while the response of the PID control system showed a large overshoot in a short time. In addition, the time of the former to the steady state was shortened by 5.619% compared with the latter. After the interference signal with a frequency of 20Hz was added, the fuzzy PID control system had a large overshoot in a short period of time compared with the PID control system. In the rest of the time, the fluctuation range of the response of the fuzzy PID control system to interference was smaller than that of the PID control system. Moreover, the response time of the fuzzy PID control system needed to reach the steady state was shortened by 16.526% when the PID control system was in a steady state. After the interference signals of 30 Hz and 40 Hz were added, the oscillation frequency of the PID control system was higher than that of the fuzzy PID control system. The time taken to reach the steady state increased by 6.157% and 6.936%, respectively. After the interference signal with a frequency of 50 Hz was added, there was little difference between the response oscillations of the two, but the response of the fuzzy PID control system to the steady state was equal to a 7.227% shorter time. Therefore, according to the simulation results, compared with the PID control system, the fuzzy PID control system had stronger stability and better ability to resist interference in the face of external vibration interference, so it was also more suitable for the field work environment.



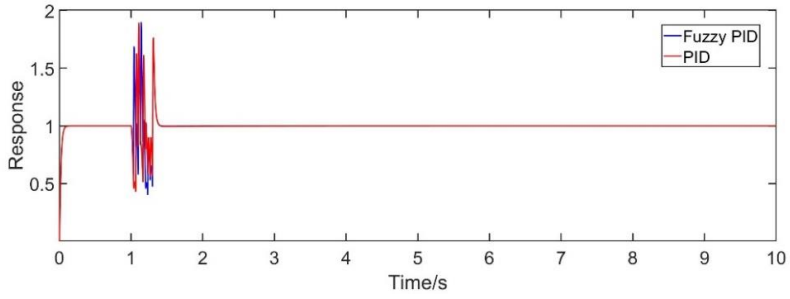
(**a**) 3 Hz



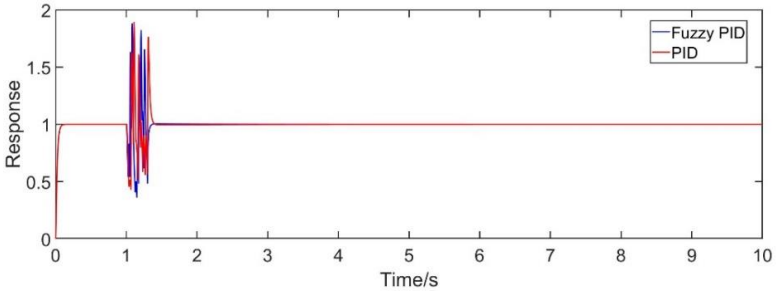
(**b**) 10 Hz



(**c**) 20 Hz

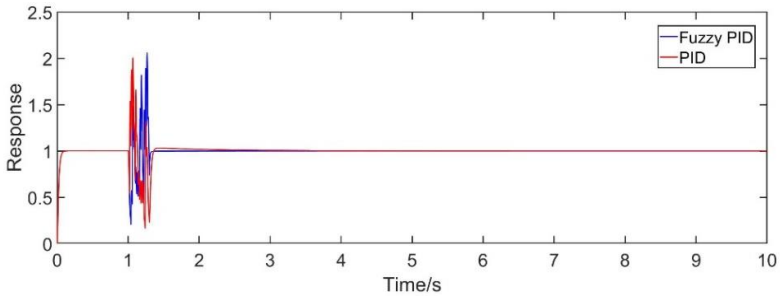


(**d**) 30 Hz



(**e**) 40 Hz

Figure 8. *Cont*.



(**f**) 50 Hz

Figure 8. Step response after adding interference. (**a**) response curve of interference signal frequency of 3Hz. (**b**) response curve of interference signal frequency of 10Hz. (**c**) response curve of interference signal frequency of 20Hz. (**d**) response curve of interference signal frequency of 30Hz. (**e**) response curve of interference signal frequency of 40Hz. (**f**) response curve of interference signal frequency of 50Hz.

5. Position Control Test of Seedling Taking Mechanism

In this test, the undersurface of the screw nut was 5 mm away from the undersurface of the upper bearing seat as the initial position of the seedling-taking mechanism; the nut of the seedling-taking mechanism was controlled by these two control systems to move the specified distance; and the distance between the two surfaces was measured by an electronic vernier caliper after each movement stops, to measure the actual displacement of the nut. Due to the limitation of the structure size of the seedling-picking mechanism itself, this test was conducted in five groups with 3 mm as a gradient to ensure the reliability of the test and to reduce the chance of occurrence during the test; each group of testing was repeated five times, and the median of these five data was taken as the final output of the actual displacement. The positioning control test stand is shown in Figure 9. The test results are shown in Table 4. The absolute error and relative error of the displacement were used to compare the difference of the control results, and the variance of actual displacement was used to compare the stability of the control system output.

$$e_j = s - x \tag{20}$$

$$\Delta e_j = \frac{e_j}{x} \tag{21}$$

$$S^2 = \frac{\sum_{i=1}^{n} (a_i - \overline{x})^2}{n} \tag{22}$$

where e_j, Δe_j, x, and s represent the absolute error, the relative error, the actual displacement, and the expected displacement, respectively; S^2, a_i, $\overline{x}$ and n are the variance, the displacement amount, the average value of the displacement amount, and the number of experimental groups of the nut's actual moving displacement, respectively. i can be replaced by 1, 2, 3... n.

As can be seen from Table 4, under the control of both control systems, although the actual displacement of the nut in the seedling-picking mechanism had some deviations compared with the expected value, these deviations were relatively small and basically met the requirements. Under the action of the PID control system, the maximum deviation of the displacement of the seedling-picking mechanism was 0.09 mm, the average relative error was 0.6202%, and the variance of the actual displacement was 18.29 mm; under the action of fuzzy PID control system, the maximum deviation of the displacement of the seedling-picking mechanism was 0.05 mm, and the average relative error was 0.3578%. The variance of the actual displacement was 18.12 mm, which was smaller than the variance of the actual displacement of the PID control system. Therefore, the fuzzy PID control system was more suitable as the control system of the seedling-picking mechanism because its

output had higher positioning accuracy and more stable output with higher reliability than the PID control system.

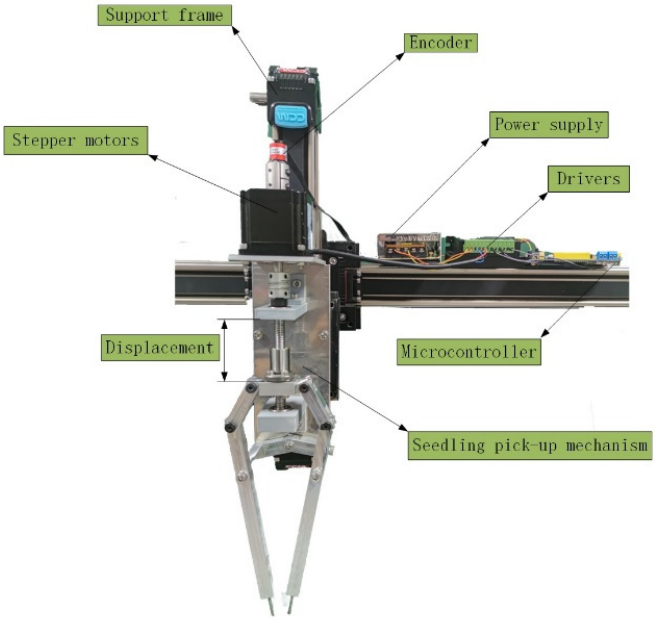


Figure 9. Positioning control test stand.

Table 4. Positioning control test results.

Test Serial Number	Expected Displacement /mm	PID Control Results			Fuzzy PID Control Results		
		Actual Displacement/mm	Absolute Error/mm	Relative Error/%	Actual Displacement/mm	Absolute Error/mm	Relative Error/%
1	5	4.91	0.09	+1.832	4.95	+0.05	+1.010
2	8	8.02	−0.02	−0.249	7.98	+0.02	+0.251
3	11	10.97	+0.03	+0.273	10.98	+0.02	+0.182
4	14	14.02	−0.08	−0.571	13.96	+0.04	−0.287
5	17	17.03	−0.03	−0.176	17.01	−0.01	+0.059

6. Conclusions

(1) In order to ensure the success rate of the pot seedling grasping and low damage rate of the pot seedling, and to achieve the high efficiency of pot seedling transplanting, and to consider the complexity of the working environment of the seedling-picking mechanism and the uncertainty of the interference, the paper adapted the control method of adding the adaptive fuzzy PID control algorithm to the control system to achieve the precise opening and closing positioning control of the seedling-picking mechanism.

(2) The simulation model of the stepper motor rotor angular velocity control system based on fuzzy PID control and traditional PID control was built in MATLAB/Simulink. The unit step response results show that the time the fuzzy PID control system took to reach the steady state was 0.145s, and the time the traditional PID control algorithm took to reach the steady state was 0.152s. The time the fuzzy PID control system took to reach the steady state was shortened by 4.61% compared with the time the traditional PID control system took to reach the steady state. In addition, on the basis of the unit step signal as an excitation signal, six groups of interference signals with different frequencies were added in the same time period. The response results show that after adding interference signals with frequencies of 3 Hz, 10 Hz, 20 Hz, 30 Hz, 40 Hz, and 50Hz, compared with the PID control algorithm, the time the fuzzy PID control algorithm took to reach the steady state was shortened by 0.318%, 5.619%, 16.526%, 6.157%, 6.936%, and 7.277%, respectively. Therefore, the simulation results show that the fuzzy PID control is more stable than the traditional PID control, and the dynamic control performance is better.

(3) The experimental platform was built, and the positioning test of the seedling-picking mechanism was carried out by using the fuzzy PID control system and the traditional PID control system. The test results show that the fuzzy PID control system has better control performance. Compared with the traditional PID control system, the fuzzy PID control system has better dynamic performance. As the formulation of fuzzy rules is only suitable for laboratory environment, the actual operation of field transplanting needs to be further verified and improved.

Author Contributions: Conceptualization, S.H. and W.W.; methodology, S.H.; software, Y.W.; validation, S.H. and G.L.; formal analysis, S.H.; investigation, S.H.; resources, S.H. and W.W.; data curation, S.H.; writing—original draft preparation, S.H.; writing—review and editing, W.W. and G.L.; visualization, S.H.; supervision, W.W. and Y.W; project administration, W.W.; and funding acquisition, W.W. All authors have read and agreed to the published version of the manuscript.

Funding: This research was funded by National Nature Fund, grant number 61763042.

Institutional Review Board Statement: Not applicable.

Informed Consent Statement: Not applicable.

Data Availability Statement: Not applicable.

Conflicts of Interest: The authors declare no conflict of interest.

References

1. Ji, J.T.; Yang, L.H.; Jin, X.; Gao, S.; Pang, J.; Wang, J.L. Design and parameter optimization of planetary gear-train type pot seedling planting mechanism. *Trans. Chin. Soc. Agric. Eng.* **2018**, *34*, 83–92.
2. Wen, Y.S.; Zhang, J.X.; Yuan, T.; Tan, Y.Z. Current situation and analysis of automatic pich-up technology for vegetable plug seedlings. *J. China Agric. Univ.* **2021**, *26*, 128–142.
3. Zhang, K.X.; Wu, H.; Wang, W.Z.; Song, C.; Liu, X.X. Design and experiment of clamping picking seedling mechanism for tomato transplanter. *J. Agric. Mech. Res.* **2020**, *42*, 64–68.
4. Hu, J.P.; Chang, H.; Yang, L.H.; Han, L.H.; Mao, H.P.; Zhang, S.W. Design and experiment of control system for automatic transplanter picking up and spacing casting whole row of seedlings. *Trans. Chin. Soc. Agric. Mach.* **2018**, *49*, 78–84.
5. Ren, L.; Wang, N.; Cao, W.B.; Li, J.Q.; Ye, X.C. Fuzzy PID control of manipulator positioning for taking the whole row seedlings of tomato plug seedlings. *Trans. Chin. Soc. Agric. Eng.* **2020**, *36*, 21–30.
6. Wang, Q.; Cao, W.B.; Zhang, Z.G.; Zhang, P.; Wang, P. Location control of automatic pick-up plug seedlings mechanism based on adaptive fuzzy-PID. *Trans. Chin. Soc. Agric. Eng.* **2013**, *29*, 32–39.
7. Liu, J.D.; Cao, W.B.; Xu, H.Z.; Tian, D.Y.; Jiao, H.B.; OuYang, Y.N. Adaptive fuzzy-PID control of accurate orientation of auto-detect seedling supply device. *Trans. Chin. Soc. Agric. Eng.* **2017**, *33*, 37–44.
8. Wang, C.L.; Yong, L.; Song, J.N.; Ma, R.H.; Liu, C.L.; Li, F.L. Design and Test of Automatic Control System of Pneumatic Ejecting Type High-Speed Transplanter. *Trans. Chin. Soc. Agric. Mach.* **2022**, *53*, 114–125.
9. Wei, X.H.; Bao, S.; Liu, X.K.; Liu, C.L.; Mao, H.P. Design and experiment on potted-seedling automatic transplanter control system for motion coordinating. *Trans. Chin. Soc. Agric. Mach.* **2016**, *47*, 52.
10. Ma, X.Y.; Sun, F.C.; Wang, Y.M.; Li, X.C.; Yuan, J. Double Closed-loop Control of Multi-leaf Collimator Based on Fuzzy Adaptive PID. *Control Eng. Chin.* **2021**, *28*, 313–318.
11. Wu, H.Y.; Shen, Q.K.; Zhang, W.X. Raw water pre-treatment system based on neural network adaptive PID control algorithm. *Therm. Power Gener.* **2018**, *47*, 41–47.
12. Yang, J.J.; He, E.; Shu, J.C. Application of adaptive fuzzy control in suppressing vibration response of offshore floating wind turbines. *J. Northwest. Polytech. Univ.* **2021**, *39*, 241–248. [CrossRef]
13. Wu, Z.Y.; Li, X.X. The application of self-tuning fuzzy PID control on non-circular cutting. *Modul. Mach. Tool Autom. Manuf. Tech.* **2020**, *11*, 120–124.
14. Lin, J.H. Comparison of Neural Network and Fuzzy Logic Control Systems. *Mech. Sci. Technol. Aerosp. Eng.* **1996**, *2*, 162–166+181.
15. Huan, Q.W.; Si, W.L.; Xue, B.Y. Adaptive neural control for non-strict-feedback nonlinear systems with input delay. *Inf. Sci.* **2020**, *514*, 605–616.
16. Gao, Z.Y. Research on Two-phase Hybrid Stepper Motor Control Based on Sliding Mode Algorithm of Time-varying Boundary Layer. *South China Univ. Technol.* **2020**. [CrossRef]
17. Wang, B.J.; Liu, Q.X.; Zhou, L.; Bu, L.; Li, X.Q.; Zhang, J.Q. Modeling of stepper motor control system and optimization of acceleration and deceleration curve. *Electr. Mach. Control* **2018**, *22*, 37–42+52.
18. Xu, G.Q.; Chen, Y.; Wang, P. Design Simulation of Hybrid Stepping Motor Fuzzy PID Controller. *J. Anhui Polytech. Univ.* **2019**, *34*, 39–45.

19. Gu, L.C.; Qi, Z.L.; Li, J.B. Research on Application of Fuzzy and PID Control in Flow Control of Variable Speed Hydraulic Power Source. *Mech. Des. Manuf.* **2021**, *4*, 29–33.
20. Wang, X.Y.; Zhao, J.F. Design and implementation of PLC based on fuzzy-PID dual motor synchronous control. *Mod. Manuf. Eng.* **2020**, 128–133.
21. Sha, Y.G.; Wang, Q.; He, X.H. Trajectory Tracking Control of Hydraulic Mechanical Arm Based on Fuzzy Compensation. *Inf. Control* **2021**, *50*, 184–194.
22. Chen, D.H.; Zhu, Z.K.; Wang, C. Hydraulic turbine set frequency control based on fuzzy neural network PID. *Mod. Electron. Tech.* **2020**, *43*, 99–102.
23. Yin, H.Q.; Yi, W.J.; Li, C.Q. Research on control system of Missile-borne brushless DC motor based on speed loop fuzzy parameter adaptive PID algorithm. *Acta Armamentarii* **2020**, *41*, 30–38.
24. Xin, J.; Kai, K.C.; Yang, Z.; Jang, T.J. Simulation of hydraulic transplanting robot control system based on fuzzy PID controller. *Measurement* **2020**, *164*, 108023.
25. Yang, J.W.; Hou, Y.L.; Li, Q.; Li, Y. Modified organophosphorus fire retardant with low toxicity/high flame retardancy using the pharmacophore model associated with Mamdani fuzzy inference approach. *Biochem. J.* **2020**, *477*, 4655–4674. [CrossRef] [PubMed]
26. Liu, L.L.; Zuo, J.H. Parameter Self-adjusting Control Method of Fuzzy PID for Magnetic Levitation Ball System. *Control Eng. China* **2021**, *28*, 354–359.
27. Chen, M.; Wang, J. Simulation system of Ziegler-Nichols PID parameter tuning based on MATLAB GUI. *Lab. Res. Explor.* **2020**, *39*, 98–101+122.